

Structure and dynamics of liquid carbon

C. Z. Wang, K. M. Ho, and C. T. Chan

Ames Laboratory and Department of Physics, Iowa State University, Ames, Iowa 50011

(Received 5 February 1993)

Structural, dynamical, and electronic properties of liquid carbon are studied by molecular-dynamics simulation with the use of a well-tested tight-binding Hamiltonian. We demonstrate that tight-binding molecular dynamics has sufficient efficiency and accuracy for a realistic simulation study of complex carbon systems. Our extensive simulation results show that liquid carbon at low density is metallic and dominated by twofold and threefold atoms. On the other hand, the high-density liquid is found to exhibit considerable diamondlike tetrahedral bonding.

I. INTRODUCTION

The liquid phase of carbon has attracted interest in the fields of condensed-matter physics, geology, and astrophysics over many years.¹ The extraordinary ability of carbon atoms to form strong chemical bonds in twofold, threefold, as well as fourfold coordinations makes the liquid phase of carbon complex and interesting. Unlike the case of liquid silicon, where the coordination number is higher than 4 (about 6.5),² the average coordination of atoms in liquid carbon is less than 4. Because the melting temperature of carbon is extremely high (about 5000 K under normal conditions),¹ it is very difficult to prepare equilibrium samples of liquid carbon in the laboratory. There has been no measurement which determines directly the structure of liquid carbon, but only indications of structural changes as graphite and diamond melt.^{1,3}

In the last several years, there has been rapid progress in the study of this complex system with realistic simulation techniques. Molecular-dynamics (MD) and Monte Carlo (MC) studies have been performed using either the Car-Parrinello scheme^{4,5} or empirical classical potentials.⁶ The Car-Parrinello method can treat the interatomic interactions accurately within the framework of *ab initio* density-functional theory with local-density approximation (LDA). However, simulation for carbon systems demands a huge plane-wave basis set in order to obtain converged results, which makes the method rather expensive for extensive simulations. The classical-potential simulations, on the other hand, can handle a larger number of atoms and longer simulation periods, but the interatomic interactions are *ad hoc* and less accurate. Also, they do not *a priori* yield information on the electronic structure of the system.

Recently, we have developed a molecular-dynamics scheme⁷ that incorporates electronic structure effects into MD simulations through a tight-binding parametrization. In this "tight-binding molecular-dynamics (TBMD)" approach, the covalent bonding of the material enters the calculations in a natural way from the underlying electronic structure rather than through *ad hoc* *N*-body potentials. Unlike the Car-Parrinello approach which relies on expansion of the electronic wave functions by plane

waves,⁴ the tight-binding electronic calculations require only a few atomic orbitals for each atom, allowing a larger number of atoms and longer simulation periods to be tackled within the present computer capabilities.

In this paper, we report an extensive simulation study of structural and electronic properties of liquid carbon using the TBMD scheme. We first tested our TBMD scheme by performing simulation of liquid carbon under similar conditions as those in Ref. 4. While obtaining very similar results, the TBMD simulation is found to be about 200 times faster than the Car-Parrinello scheme. With such an accuracy and efficiency, we performed further simulations to study the structure of the liquid at various densities. We also investigated the effects of the size of the unit cell used in the simulations. We found that while the structure of the liquid is less sensitive to the size and orientation of the unit cell, it is very sensitive to the density of the sample. Our study provides insight into the structure of liquid carbon and suggests that the "carbyne" phase may be stable in the high-temperature and low-density regime, while tetrahedral-bonded liquid may exist at high densities. Our study also demonstrates that the TBMD scheme can bridge the gap between the Car-Parrinello and classical-potential approaches and has sufficient accuracy and efficiency for a realistic simulation study of the structural and electronic properties of complex carbon systems.

II. TIGHT-BINDING ENERGY MODEL FOR CARBON

In our tight-binding molecular-dynamics scheme,⁷ the system is described by a Hamiltonian of the form

$$H(\{\mathbf{r}_i\}) = \sum_i \frac{\mathbf{P}_i^2}{2m} + \sum_n^{\text{occupied}} \langle \psi_n | H_{\text{TB}}(\{\mathbf{r}_i\}) | \psi_n \rangle + E_{\text{rep}}(\{\mathbf{r}_i\}), \quad (1)$$

where $\{\mathbf{r}_i\}$ denotes the positions of the atoms ($i = 1, 2, \dots, N$) and \mathbf{P}_i denotes the momentum of the *i*th atom. The first term in (1) is the kinetic energy of the ions, the second term is the electronic band-structure en-

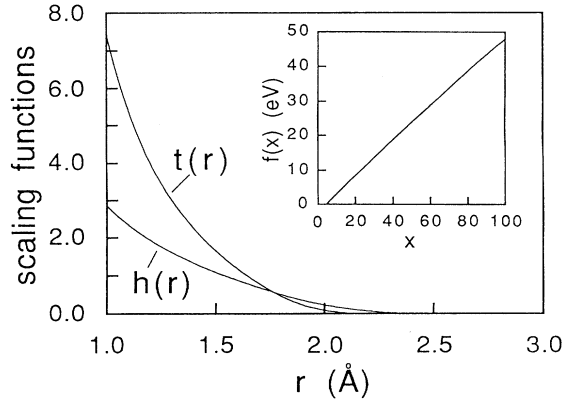


FIG. 1. Scaling functions of the tight-binding potential model. See text and Ref. 8 for the details.

ergy calculated from a parametrized tight-binding Hamiltonian $H_{TB}(\{\mathbf{r}_i\})$, and the third term is a short-ranged repulsive energy. In this scheme, electronic degrees of freedom are explicitly involved in the force calculation but not in the dynamics. The former feature places the scheme within the quantum-mechanics regime, while the latter allows the simulation to use time steps about 10 times larger than that used in the Car-Parrinello scheme.

The tight-binding model used in the present simulation consists of an orthogonal sp^3 basis with on-site atomic energies $\varepsilon_s = -2.99$ eV and $\varepsilon_p = 3.71$ eV and two-center integrals $V_{ss\sigma}(r) = -5.00h(r)$ eV, $V_{sp\sigma}(r) = 4.70h(r)$ eV, $V_{pp\sigma}(r) = 5.50h(r)$ eV, and $V_{pp\pi}(r) = -1.55h(r)$ eV, where $h(r)$ is a smooth function of interatomic distance as shown in Fig. 1. The repulsive energy is in the form of $E_{rep} = \sum_i f[\sum_j \phi(r_{ij})]$, where $\phi(r_{ij}) [=8.18555t(r_{ij})]$ eV is a pairwise repulsive interaction and f is a functional with argument $x = \sum_j \phi(r_{ij})$. The function $t(r)$ and the functional $f(x)$ are also plotted in Fig. 1. More details about the tight-binding model can be found in Ref. 8. The accuracy and transferability of this model have been well tested. It reproduces well the first-

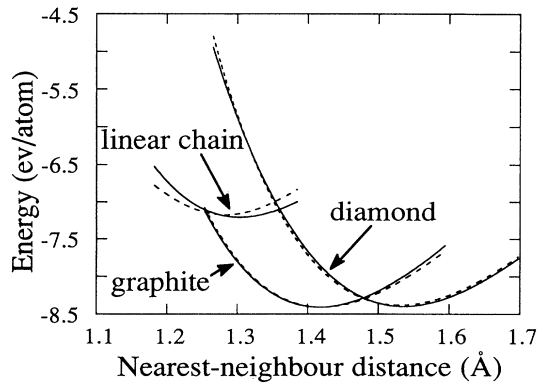


FIG. 2. Binding energies as a function of nearest-neighbor distance for carbon in diamond, graphite, and linear chain structures. Solid and dashed lines show the results from tight-binding and LDA calculations, respectively.

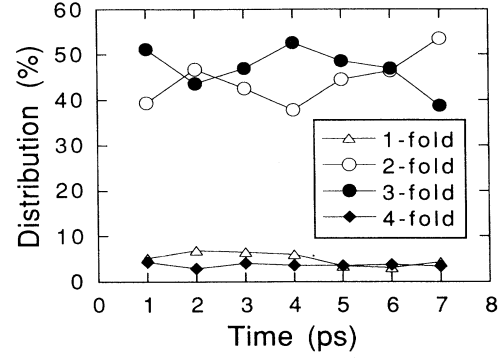


FIG. 3. Distribution of various coordinated atoms in liquid carbon as a function of time. Each point represents an average value (percentage) over 1 ps.

principles-calculated energy versus volume curves for various coordinated crystalline structures of carbon. In particular, the energy curves of the linear chain (twofold), graphite (threefold), and diamond (fourfold) structures are excellently described, as one can see from Fig. 2. The model also describes well the elastic, vibrational, and anharmonic properties of diamond and graphite, as well as the properties of more complex systems such as carbon clusters with sizes ranging from 5 atoms to 100 atoms.⁸⁻¹⁰

III. SIMULATIONS AND RESULTS

A. Low-density liquids

Using the tight-binding model as described in the previous section, we first performed a simulation with a 54-

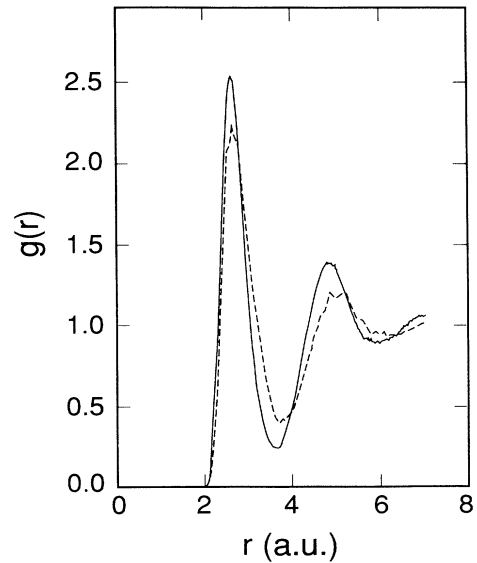


FIG. 4. Pair-correlation function $g(r)$ of liquid carbon obtained from TBMD (solid line) is compared with the *ab initio* MD result of Ref. 4 (dashed line). Both simulations used 54 atoms.

atom unit cell and with fcc periodic boundary conditions. The density of the sample was chosen to be 2.0 g/cm^3 . These conditions are the same as those used in the *ab initio* MD study of Ref. 4. Our simulation was initiated with all atoms arranged in the diamond lattice. The equations of motions of the atoms were solved by the fifth-order predictor-corrector algorithm with a time step of $0.7 \times 10^{-15} \text{ s}$. Stochastic temperature control¹¹ was used to thermalize the system. The temperature of the system is increased at a rate of 300 K every $7 \times 10^{-14} \text{ s}$ after Ref. 4. The expanded diamond crystal at such a low density was found to be unstable towards lower-coordinated structures already at low temperature ($T \leq 500 \text{ K}$). We heated the system up to about 5000 K and studied the liquid properties at that temperature. After 0.21 ps of thermalization at 5000 K, statistical averages for the structural properties were computed for every picosecond over a total of 7 ps. In Fig. 3, the distributions of various coordinated atoms obtained from these seven runs are plotted. We found that the liquid structure at this density regime is dominated by twofold and threefold atoms. We also noted that the fluctuation in the atomic distributions is quite large (about 10%). With such a small unit cell, a statistical average performed over more than 5 ps is necessary to get converged results. By taking the statistical average over 7 ps of simulation time, we estimated that the liquid carbon at this density contains $5.1 \pm 1.5\%$ of onefold, $44.4 \pm 5.2\%$ of twofold, $46.9 \pm 4.7\%$ of threefold, and $3.6 \pm 0.5\%$ of fourfold atoms, respectively. We have tested and found that the above results are not sensitive to the details of the simulation (e.g., different thermalization steps, different ensemble averaging, etc.; see also Table I). The pair-correlation functions $g(r)$ obtained from our simulation is compared with that from the *ab initio* MD of Ref. 4 as plotted in Fig. 4. Our simulation results are in general similar to the *ab initio* MD results of Ref. 4. However, there are some subtle differences in the distribution of the various coordinated atoms in the liquid structure. In particular, we found more twofold atoms and fewer fourfold atoms. We also found the presence of onefold atoms, which indicates the presence of dimer and trimer species in the liquid phase in this density regime. No detailed experimental data on the structure of the liquid carbon are available for comparison with the theoretical results.

We have also performed simulations under the same density (2.0 g/cm^3) but using 64-atom and 216-atom unit cells, respectively, with cubic periodic boundary condi-

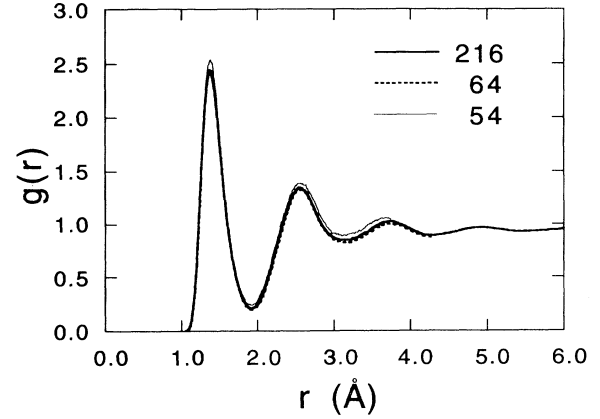


FIG. 5. Comparison of pair-correlation functions of liquid carbon obtained by using different sizes of unit cells. The density of the samples is 2.0 g/cm^3 .

tions, in order to test the effects of size and orientation of the unit cell on the liquid structure. The results of pair-correlation functions and atomic distributions obtained from different sizes are compared in Fig. 5 and Table I. These results show that the size effects on the liquid structure are small.

To further characterize the structure of the liquid, we have plotted in Figs. 6 and 7 the partial radial distribution functions and the bond-angle distribution functions of various coordinated atoms, respectively. The results show that the average bond length between twofold atoms is slightly smaller than that between threefold atoms. There are considerable numbers of threefold atoms surrounding the twofold atoms as indicated by the peaks of $g_{23}(r)$. Our results also show that while the bond angles between threefold atoms are centered at 120° , those of the twofold atoms favor a linear arrangement. We note that the bond-angle distribution of the twofold atoms, A_{22} , is also different from that of Ref. 4, in which A_{22} is basically uniformly distributed over a very wide range of angles.⁴

We have also studied the dynamical properties of the liquid by calculating the atomic diffusion constant, which is estimated from the time dependence of the mean-square displacement, $\langle R^2(t) \rangle = \langle N^{-1} \sum_{i=1}^N |\mathbf{R}_i(t + \tau) - \mathbf{R}_i(\tau)|^2 \rangle_\tau$. The result of $\langle R^2(t) \rangle$ as a function of time t obtained from the 216-atom sample is plotted in Fig. 8.

TABLE I. Ratios of various coordinated atoms of liquid carbon under density of 2.0 g/cm^3 . The TBMD results obtained by using 216-atom (TB-216), 64-atom (TB-64), and 54-atom (TB-54) unit cells are compared with the results of *ab initio* MD simulation of Ref. 4 (CP-54). n_c is the average coordination number. D is the diffusion constant.

Sample	Onefold (%)	Twofold (%)	Threefold (%)	Fourfold (%)	n_c	D ($10^{-4} \text{ cm}^2 \text{ s}^{-1}$)
TB-216	4.6 ± 0.5	43.2 ± 2.5	48.1 ± 2.0	4.1 ± 0.5	2.4	2.05
TB-64	4.0 ± 0.5	42.2 ± 2.5	50.0 ± 2.2	3.8 ± 0.5	2.4	1.70
TB-54	4.8 ± 0.5	43.2 ± 5.5	48.0 ± 5.0	4.0 ± 0.7	2.4	
CP-54	0.0	32.0	52.0	16.0	2.9	2.40

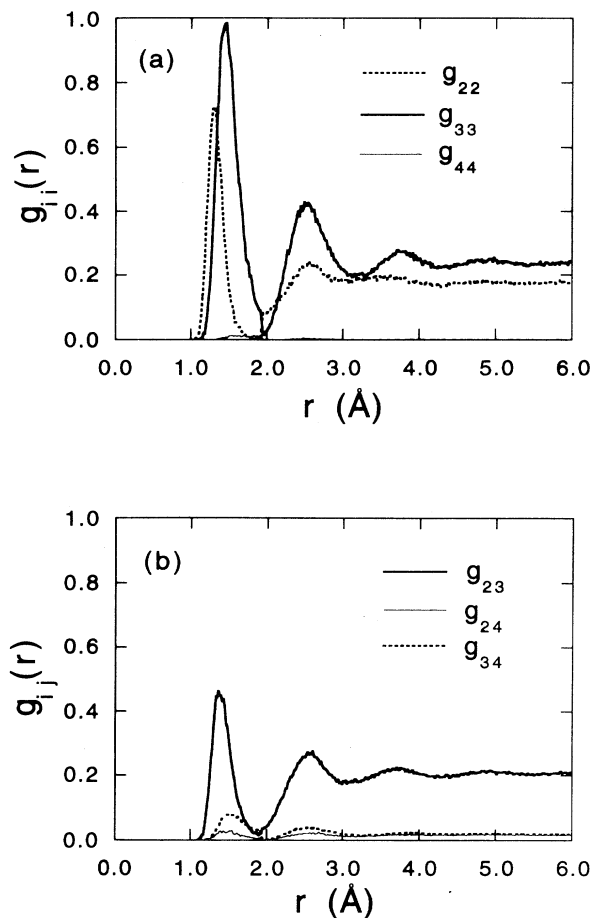


FIG. 6. Partial radial distribution functions of liquid carbon. The unit cell size is 216 atoms and the density is 2.0 g/cm^3 .

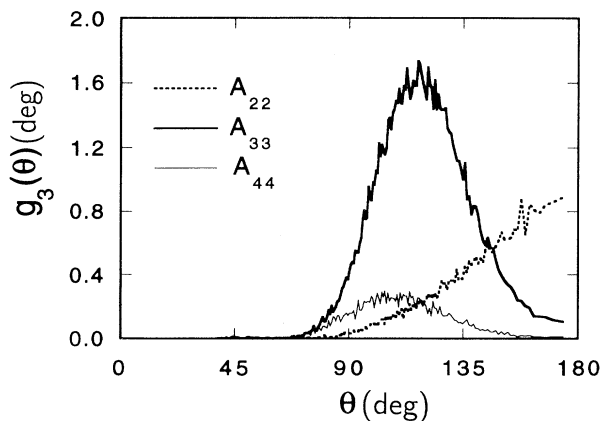


FIG. 7. Angular distribution functions of liquid carbon. The unit cell size is 216 atoms and the density is 2.0 g/cm^3 .

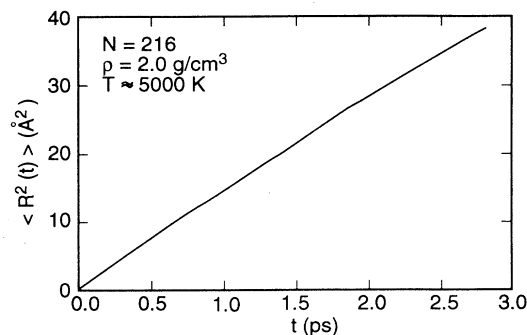


FIG. 8. Mean-square displacement of carbon atoms in the liquid carbon is plotted as a function of time. The result is obtained by using a 216-atom unit cell.

By using the Einstein relation $D = \lim_{t \rightarrow \infty} [\langle R^2(t) \rangle / 6t]$, we deduce the diffusion constant to be $2.05 \times 10^{-4} \text{ cm}^2/\text{s}$. This value is close to but slightly smaller than the value of $2.40 \times 10^{-4} \text{ cm}^2/\text{s}$ estimated by Galli *et al.*⁴

In the last two decades, there has been considerable debate about whether chainlike structures (so-called “carbyne” phase) exist at high temperatures and low densities^{12–16} and whether the liquid phase in this regime is insulating or metallic.^{17–21} From our simulation as discussed above, we already see that the liquid structure contains many twofold atoms. To further clarify the issue, we performed simulations at even lower densities (from 2.0 to 1.2 g/cm^3). We found that as the density becomes lower, the percentage of the twofold and onefold atoms increases rapidly. This tendency is clearly seen from Table II. Snapshot pictures of the atomic configurations as a function of density (Fig. 9) also show that

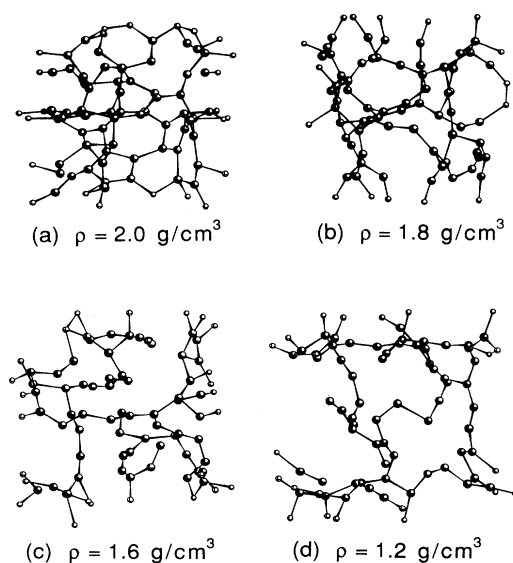


FIG. 9. Atomic configurations (snapshots) of liquid carbon at different densities.

TABLE II. Ratios of various coordinated atoms of liquid carbon as a function of density. n_c is the average coordination number.

Density (g/cm^3)	Onefold (%)	Twofold (%)	Threefold (%)	Fourfold (%)	n_c
2.68	0.8	16.9	69.1	13.2	3.0
2.44	1.6	26.3	62.1	10.0	2.8
2.0	4.0	42.0	50.0	3.8	2.4
1.8	5.5	50.8	41.8	1.9	2.4
1.6	7.6	56.9	34.0	1.5	2.3
1.2	11.0	68.0	20.0	0.7	2.1

chainlike structure becomes more and more dominant as the density is lowered. The liquids at all these densities exhibit metallic behavior as one can see from Fig. 10, where considerable electronic states are present at the Fermi level.

B. High-density liquid

The simulation for high-density liquid carbon is carried out with a 64-atom cubic cell at a fixed density of $4.4 \text{ g}/\text{cm}^3$. The simulation is initiated with all atoms arranged in the diamond lattice. We found that the diamond structure at such a high density is very difficult to melt. In Fig. 11, the total energy of the system during the heating and cooling process is plotted. Each point is an average value of 2000 MD steps after 2000 MD steps of thermalization at a given temperature. Because of the superheating and supercooling associated with the finite size and finite simulation time, we did not attempt to estimate the melting temperature. The liquid properties are studied at about 8000 K on cooling from the hot liquid. After very long thermal equilibrium runs (about 20000 steps) at this temperature, 8000 MD trajectories are used for the statistical average. We found that the

structure of liquid carbon at high density is qualitatively different from that of a low-density liquid. The radial distribution function as plotted in Fig. 12 shows a strong second-neighbor peak in addition to the nearest-neighbor peak. This feature is similar to the *ab initio* MD result of Ref. 5. Detailed analysis shows that the high-density liquid carbon obtained from our simulation is dominated by fourfold atoms (59%) and threefold atoms (38%). There are also some twofold and fivefold atoms. The average coordination number is about 3.6. In comparison, the *ab initio* MD simulation of Galli *et al.*⁵ is reported to have many more fivefold atoms (about 25%) under the same density. Our results are in qualitative but not quantitative agreement with the results of Ref. 5. In Fig. 13, the angular distribution functions of the threefold and fourfold atoms in the high-density liquid are plotted. The results show that there is a considerable amount of diamondlike tetrahedral bonding in the liquid. The electronic density of states as shown in Fig. 14 indicates that high-density liquid carbon is also metallic, although a shallow valley starts to appear at the Fermi level. Finally, from the mean-square displacement versus time plot of Fig. 15, we deduce the diffusion constant at 8000 K to be $0.3 \times 10^{-4} \text{ cm}^2/\text{s}$, which is about an order of magnitude smaller than that of the low-density liquid.

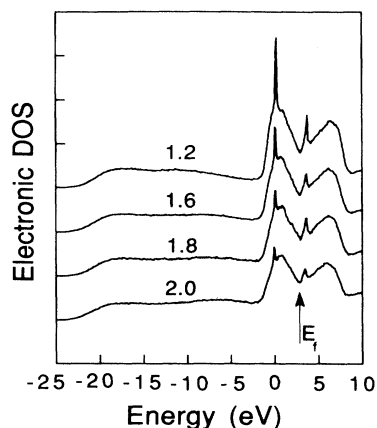


FIG. 10. Electronic density of states of liquid carbon at different densities as indicated by the numbers (in units of g/cm^3).

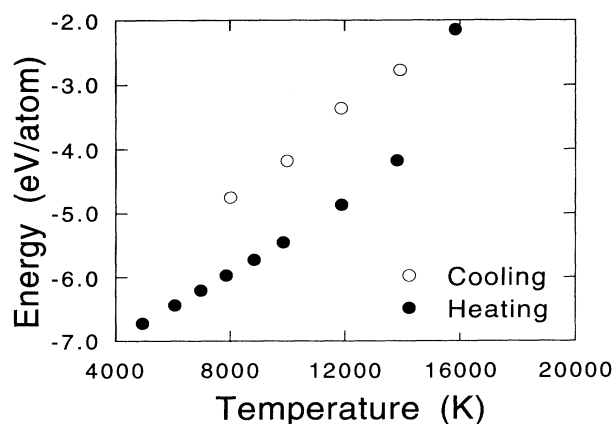


FIG. 11. Energy (per/atom) as a function of temperature for high-density ($4.4 \text{ g}/\text{cm}^3$) carbon in diamond and liquid structures.

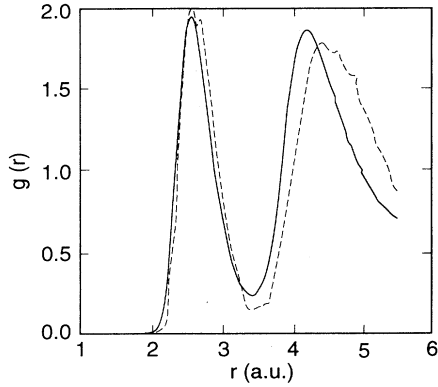


FIG. 12. Pair-correlation function $g(r)$ of high-density liquid carbon obtained from TBMD (solid line) is compared with the *ab initio* MD result of Ref. 5 (dashed line). Both simulations use a 64-atom unit cell with density of 4.4 g/cm^3 .

IV. CONCLUDING REMARKS

We have shown that the TBMD is a very efficient scheme for studying the structural, dynamical, and electronic properties of complex systems such as liquid carbon. Our simulation results in general agree well with the *ab initio* MD results. The origins of some small discrepancies are not yet clear. We note that our tight-binding model as discussed in Sec. II describes very accurately the energies of linear carbon chain, diamond as well as graphite structure in comparison with converged first-principles LDA calculation results. It is possible that the discrepancies may be partially attributed to the slightly different simulation conditions (starting configuration, simulation steps, temperature, etc.) and possible different ways of data analysis between the two simulations. Another factor that should not be overlooked is the convergence of the *ab initio* MD simulation with re-

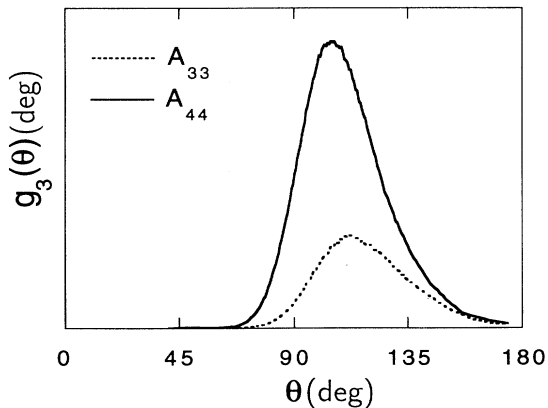


FIG. 13. Angular distribution functions of high-density (4.4 g/cm^3) liquid carbon. The results are obtained by using a 64-atom unit cell.

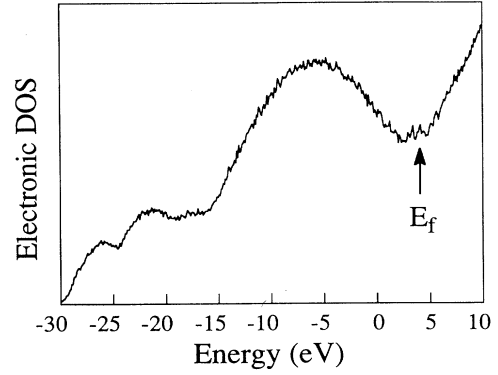


FIG. 14. Electronic density of states of high-density (4.4 g/cm^3) liquid carbon. The result is obtained by using a 64-atom unit cell. The average is performed over 8000 trajectories.

spect to plane-wave basis set used in the calculations. We hope this issue can be clarified in future studies.

The existence of the “carbyne” structure has been speculated for many years.^{12–16} Our simulation results suggest that the “carbyne” structure may be stable at very high temperatures and very low densities (about 1.0 g/cm^3). In fact, our recent simulation study on carbon fullerenes also observes chainlike structures when fullerene molecules disintegrate at high temperatures.

Carbon is a unique element of interest in many fields of science. Nevertheless, the phase diagram of carbon is still not completely determined despite considerable scientific efforts over more than 100 years. In particular, the structure of carbon in the very-high-pressure and very-high-temperature regime is still poorly understood. Our study shows that the liquid structure of carbon in this regime is very different from that at low density. With its efficiency and accuracy, our TBMD scheme is expected to play an important role in investigating various interesting yet complicated properties of carbon.

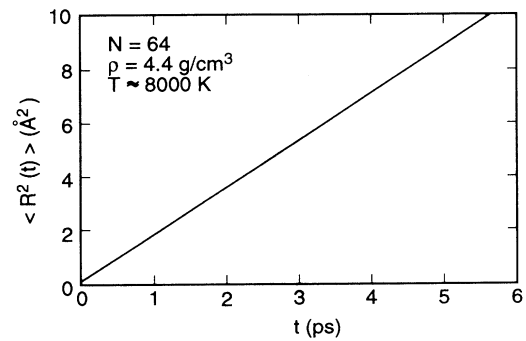


FIG. 15. Mean-square displacement of carbon atoms in the high-density liquid carbon (4.4 g/cm^3) is plotted as a function of time. The result is obtained by using a 64-atom unit cell.

ACKNOWLEDGMENTS

This work is supported by the Director of Energy Research, Office of Basic Energy Sciences. Ames Laboratory is operated for the U.S. Department of Energy by Iowa State University under Contract No. W-7405-ENG-82.

-
- ¹For a review, see, for example, F. P. Bundy, J. Geophys Res. **85**, 6930 (1985); Physica A **156**, 169 (1989).
²Y. Waseda and K. Suzuki, Z. Phys. B **20**, 339 (1975).
³D. H. Reitze, H. Ahn, and M. C. Downer, Phys. Rev. B **45**, 2677 (1992).
⁴G. Galli, R. M. Martin, R. Car, and M. Parrinello, Phys. Rev. Lett. **63**, 988 (1989); Phys. Rev. B **42**, 7470 (1990).
⁵G. Galli, R. M. Martin, R. Car, and M. Parrinello, Science **250**, 1547 (1990).
⁶J. Tersoff, Phys. Rev. Lett. **61**, 2879 (1988); Phys. Rev. B **44**, 12039 (1991).
⁷C. Z. Wang, C. T. Chan, and K. M. Ho, Phys. Rev. B **39**, 8586 (1989); Phys. Rev. Lett. **66**, 189 (1991).
⁸C. H. Xu, C. Z. Wang, C. T. Chan, and K. M. Ho, J. Phys. Condens. Matter **4**, 6047 (1992).
⁹C. Z. Wang, C. H. Xu, B. L. Zhang, C. T. Chan, and K. M. Ho, in *Physics and Chemistry of Finite Systems: From Cluster to Crystals*, edited by P. Jena, S. N. Khanna, and B. K. Rao (Kluwer Academic, Boston/London, 1992), p. 1391.
¹⁰B. L. Zhang, C. Z. Wang, and K. M. Ho, Chem. Phys. Lett. **193**, 225 (1992).
¹¹H. C. Andersen, J. Chem. Phys. **72**, 2384 (1980).
¹²A. El Goresy and G. Donnay, Science **161**, 363 (1968).
¹³A. M. Sladkov and Yu. P. Koudrayatsev, Priroda **5**, 37 (1969).
¹⁴A. G. Whittaker, Science **200**, 763 (1978); **229**, 485 (1985).
¹⁵P. P. K. Smith and P. R. Buseck, Science **216**, 985 (1982); **229**, 486 (1985).
¹⁶R. B. Heimann, J. Kleiman, and N. M. Salansky, Nature (London) **306**, 164 (1983).
¹⁷A. M. Malvezzi, N. Bloembergen, and C. Y. Huang, Phys. Rev. Lett. **57**, 146 (1986).
¹⁸E. A. Chauchard, C. E. Lee, and C. Y. Huang, Appl. Phys. Lett. **50**, 812 (1987).
¹⁹J. Heremans, C. H. Olk, G. L. Eeseley, J. Steinbeck, and G. Dresselhaus, Phys. Rev. Lett. **60**, 452 (1988).
²⁰J. Steinbeck, G. Braunstein, M. S. Dresselhaus, T. Venkatesan, and D. C. Jacobson, J. Appl. Phys. **58**, 4374 (1985).
²¹A. Ferraz and N. H. March, Phys. Chem. Liq. **8**, 289 (1979).